Bilag 2 - Chemical phosphorus (P) mapping in wastewater treatment plants (WWTPs) towards efficient P recovery

Qian Wang and Ulla Gro Nielsen, University of Southern Denmark

1. WWTPs sampling and analyses

This project investigated six WWTPs in Denmark with the sampling date given in parentheses: Ejby Mølle WWTP (June 8th, 2021), Billund WWTP (February 9th, 2021), Esbjerg WWTP (April 7th, 2021), Arla WWTP (September 28th, 2021), Biofos WWTP (November 8th, 2021), and Fredericia WWTP (January 19th, 2022).

All are municipal WWTPs except Arla, which treats dairy-processing wastewater. Sludge was sampled throughout the six WWTPs, including primary sludge (incoming P), sludge after the important treatment stages such as aeration, anaerobic digestion, and thermal hydrolysis, and final sludge at the end (outcoming P). Details of the sample locations are shown in Fig. 1. The sample ID combines the initials of the sludge type and the WWTP name.

To understand the detailed P speciation, the sludge samples were analyzed by a variety of analytical techniques. The protocol for the processing of the sludge samples and the analytical methods are described in detail in Wang et al. (2021). The results presented below for Ejby Mølle, Billund and Esbjerg WWTPs were recently reported(Wang et al., 2022)

- Bulk analysis of the whole sludge sample was performed to obtain fundamental information, e.g., organic content by loss on ignition (LOI) and elemental composition by inductively coupled plasma-optical emission spectroscopy (ICP-OES).
- The P minerals in sludge were qualitatively examined by optical microscopy, powder X-ray diffraction (PXRD), scanning electron microscopy (SEM) coupled with energy dispersive X-ray spectroscopy (EDS).

- The different P species, including inorganic orthophosphate (ortho-P), organophosphate (organic-P), pyrophosphate (pyro-P), and polyphosphate (poly-P, produced by poly-P accumulation organisms (PAOs)), were quantified using liquid-state ^{31}P nuclear magnetic resonance (NMR) spectroscopy. Selected sludge from Esbjerg, Ejby Mølle and Billund were also analyzed by solid-state ^{27}Al magic angle spinning (MAS) NMR to probe how Al affected the P speciation in the sludge.
- The different P fractions of inorganic ortho-P (e.g., vivianite-P, Fe(III)-P, Al-P, and Ca-P) were quantified by sequential P extraction.

a: Ejby Mølle

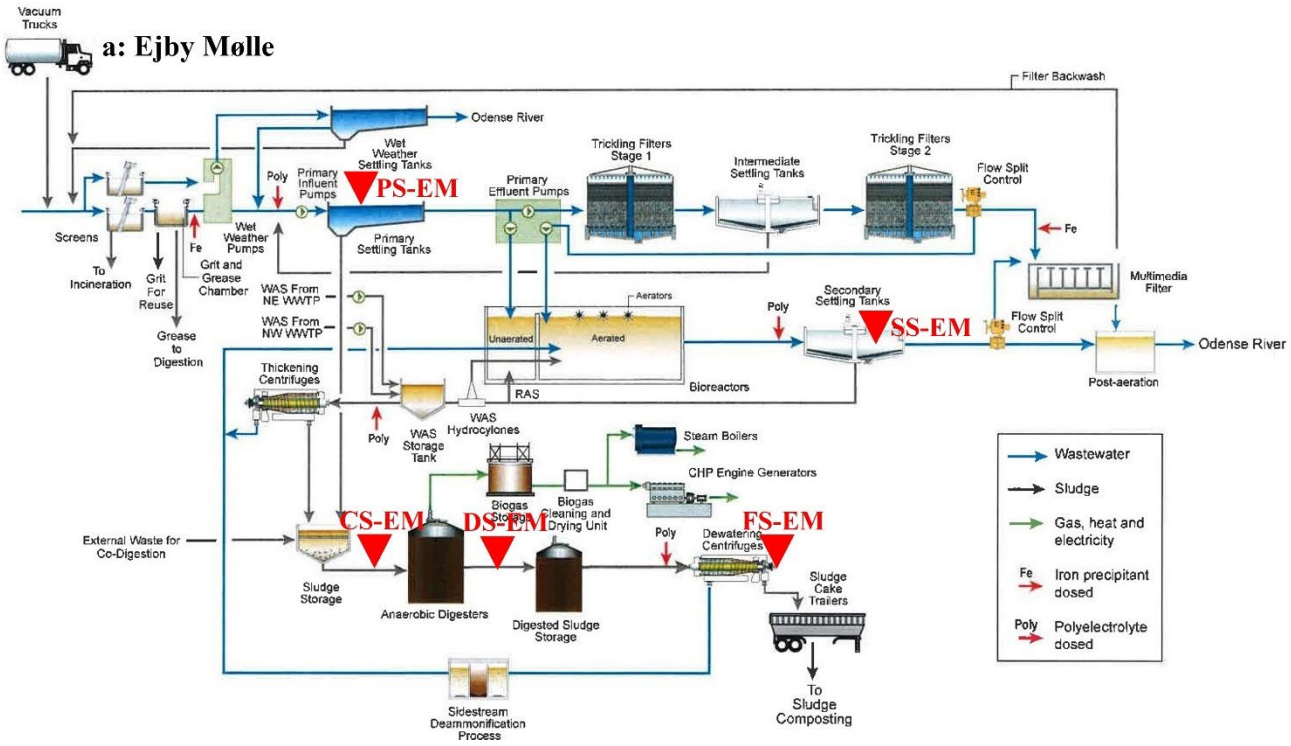

b: Billund

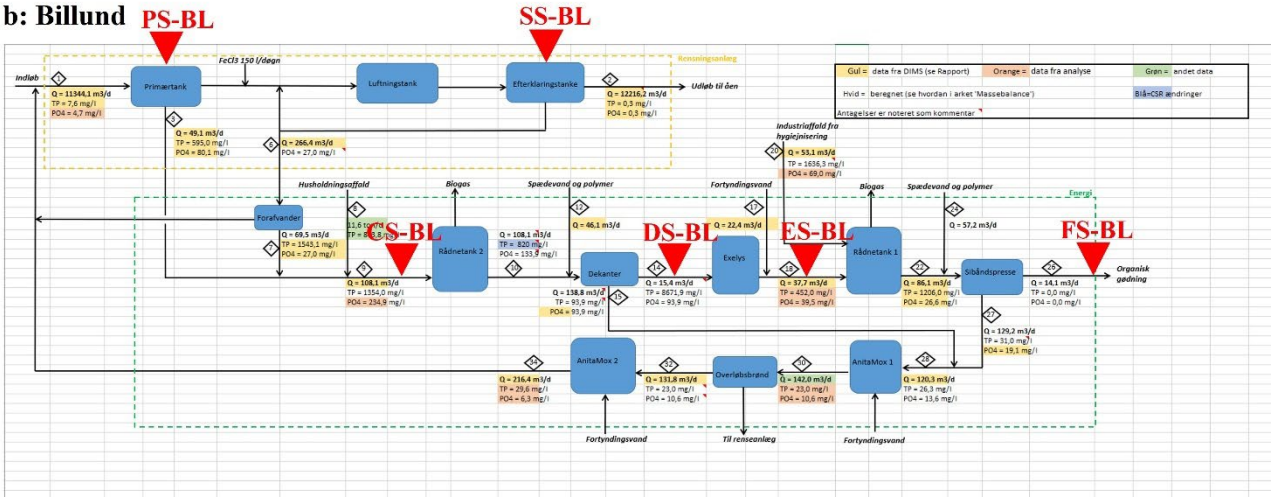

c: Esbjerg

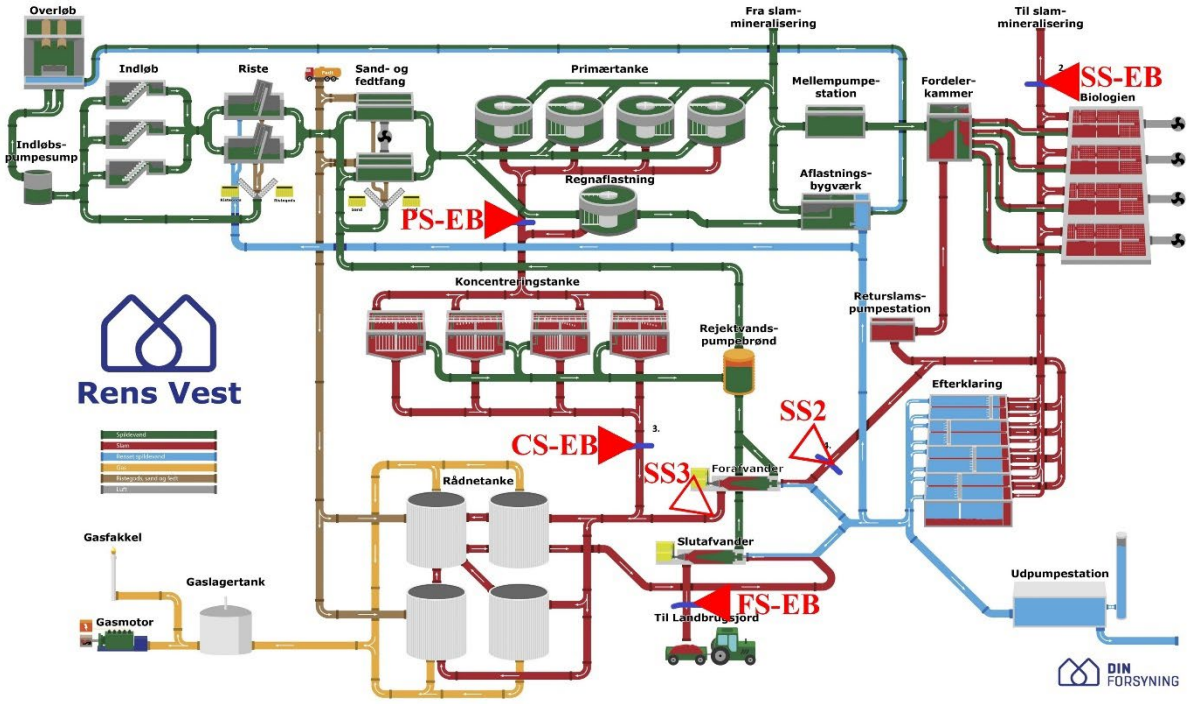

d: Arla

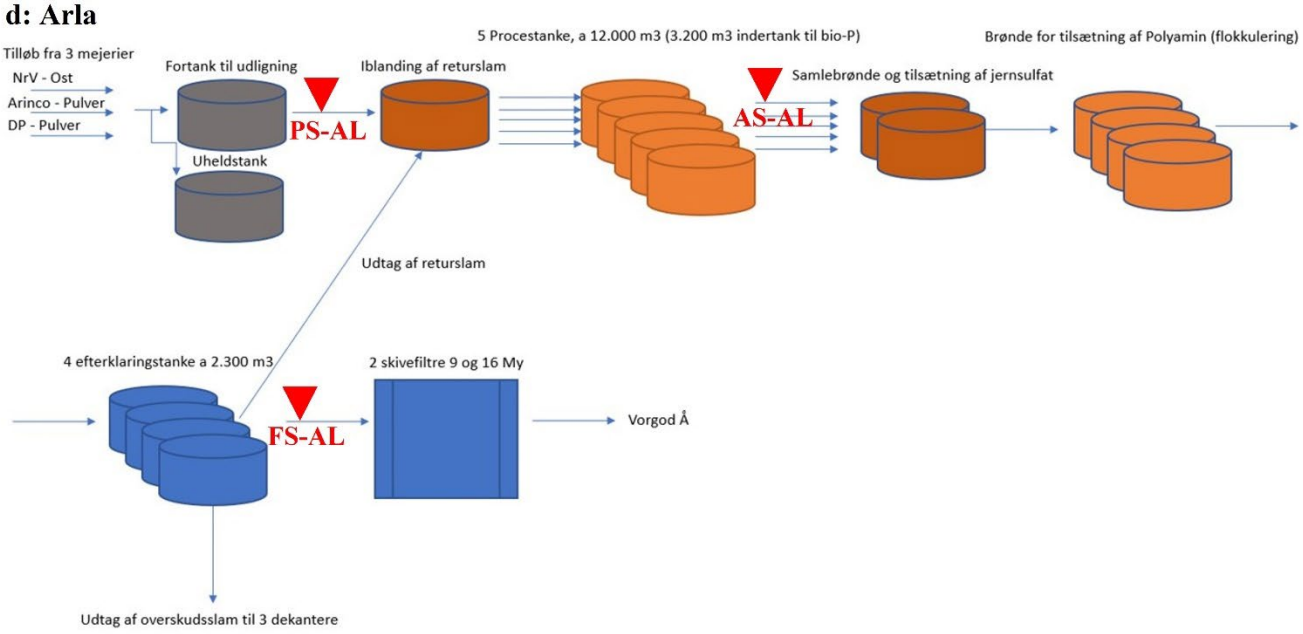

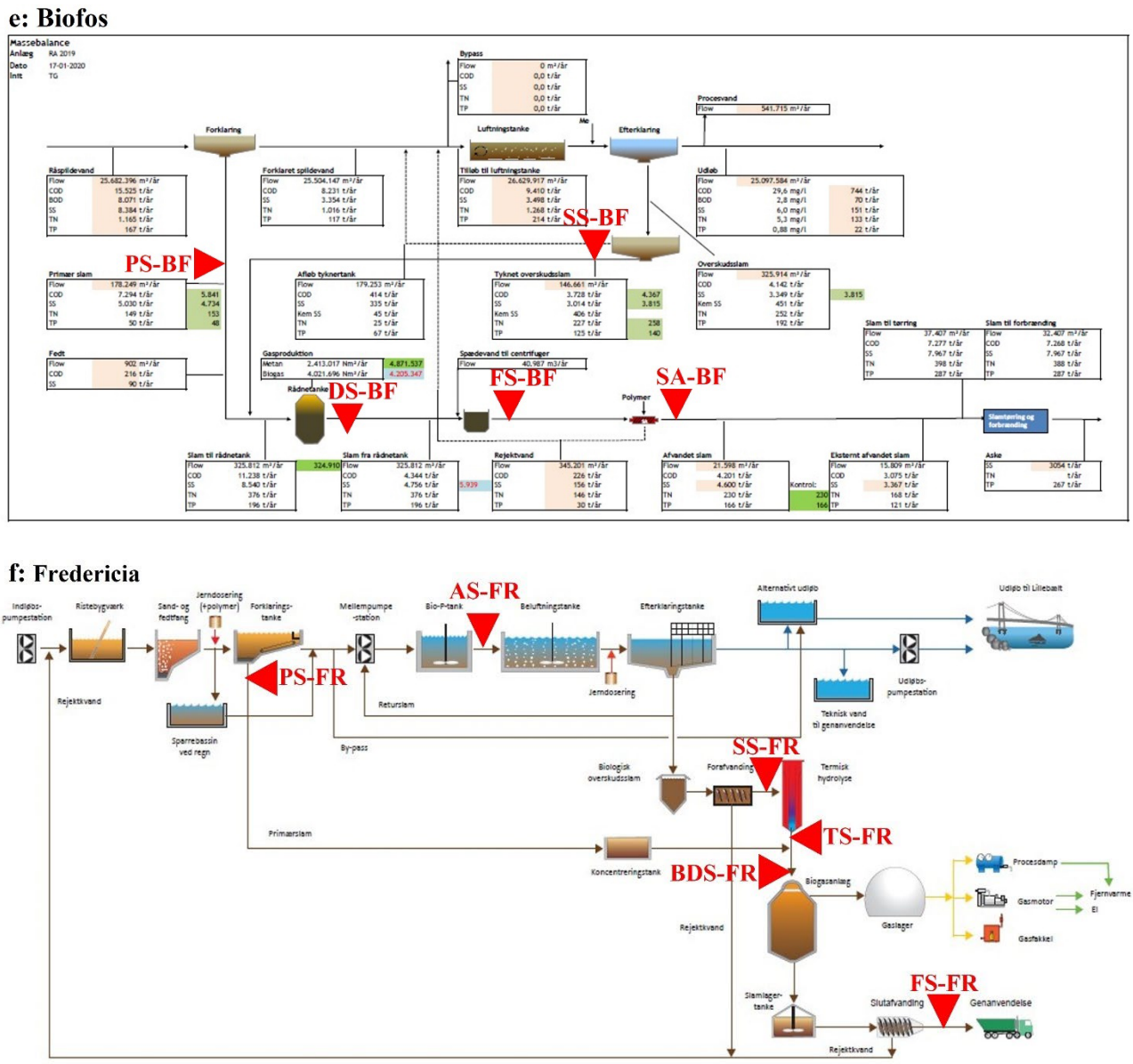

Fig. 1. Schematic diagrams of the main processes at (a) Ejby Mølle, (b) Billund, (c) Esbjerg, (d) Arla, (e) Biofos, and (f) Fredericia WWTPs with the sample location and ID indicated. EM: Ejby Mølle, BL: Billund, EB: Esbjerg, AL: Arla, BF: Biofos, FR: Fredericia, PS: primary sludge, AS: activated sludge, SS: secondary sludge, CS: sludge from concentration tank, TS: thermal hydrolysis sludge, BDS: sludge before digestion, DS: digested sludge, ES: Exelys^{TM} sludge, FS: final sludge, SA: sludge ash. At Esbjerg, two other sludge samples (SS2 and SS3 in Fig. 1c) were also collected, but they are presented, since their P speciation resembles SS-EB.

2. Characterization of the sludge samples

2.1. Elemental composition: P, Fe, and Ca are the major "inorganic" elements in the sludge

The loss on ignition (LOI, organic content) and the contents of the element phosphorus (P), iron (Fe), aluminum (Al), calcium (Ca), magnesium (Mg), and manganese (Mn), which are relevant for the P speciation in sewage sludge, are summarized in Table 1. LOI reflects the organic content of the sludge samples (based on dry weight), which decreased after anerobic digestion. All samples had a significant (60-90%) organic content except for sludge ash from Biofos (SA-BF; <1%).

As shown in Fig. 2, P, Fe, and Ca were the main elements in all sludge samples. Their contents in sludge increased after anaerobic digestion, and this should be due to that: (1) more P, Fe, and Ca precipitated from the liquid phase into the solid part via chemical and/or biological reactions during anaerobic digestion, and (2) the inorganic content was increased after the degradation of organic matter via anaerobic digestion. Given Al dosing prior to the secondary tank at Esbjerg, much higher Al contents were detected in SS-EB (21 mg/g) and FS-EB (31 mg/g) than for sludge samples without Al dosing, e.g., PS-EB (5 mg/g), CS-EB (7 mg/g), Ejby Mølle sludge (3-6 mg/g), Billund sludge (2-5 mg/g), and Arla sludge (0.1-0.7 mg/g), see Table 1. The presence of Mn in the sludge samples will be disregarded in the following discussion given its low content (< 1 mg/g). It is noted that the P content determined for the primary sludge from Fredericia significantly exceeds the other municipal WWTPs (Table 1). Moreover, the total P (TP) value based on sequential P extraction is only 14.5 mg/g, whereas 31 mg/g was determined by ICP-OES. This could be due to an experimental error or the existence of a P phase, which was not extracted by the sequential P extraction protocol. However, this P phase was dissolved by the acid digestion used prior to ICP-OES thereby explaining the discrepancy between ICP-OES and the sequential P extraction.

Table 1 Bulk analysis of the sludge samples. LOI and elemental composition are based on dry weight.

	LOI (%)	P (mg/g)	Fe (mg/g)	Ca (mg/g)	Al (mg/g)	Mg (mg/g)	Mn (mg/g)
PS-EM	74±0.2	9.2±0.09	15.6±0.02	21.4±0.04	4.7±0.00	1.8±0.00	0.31±0.00
SS-EM	73±0.2	39.8±0.28	32.0±0.05	23.8±0.05	2.9±0.03	6.5±0.00	0.34±0.00
CS-EM	73±0.3	16.6±0.21	21.1±0.06	21.0±0.06	3.9±0.00	2.8±0.00	0.32±0.01
DS-EM	58±0.6	34.8±0.11	39.9±0.04	36.1±0.15	5.5±0.04	5.4±0.03	0.62±0.00
FS-EM	60±0.3	34.5±0.05	42.8±0.22	36.6±0.14	5.3±0.05	5.5±0.02	0.66±0.00
PS-BL	87±0.1	10.4±0.05	10.6±0.10	16.0±0.00	2.5±0.01	1.8±0.01	0.42±0.002
SS-BL	87±0.0	19.4±0.03	16.5±0.03	7.1±0.01	1.9±0.03	2.9±0.01	0.18±0.003
CS-BL	89±0.2	10.8±0.06	8.0±0.00	10.9±0.01	1.9±0.04	1.6±0.00	0.16±0.000
DS-BL	71±0.2	24.6±0.06	29.0±0.18	27.1±0.04	4.0±0.01	4.7±0.03	0.39±0.002
ES-BL	64±0.1	30.7±0.06	38.8±0.17	35.6±0.11	5.1±0.01	5.8±0.02	0.51±0.003
FS-BL	64±0.4	29.1±0.09	58.6±0.03	32.8±0.09	3.8±0.01	4.1±0.01	0.51±0.003
PS-EB	85±0.0	9.9±0.06	6.5±0.04	13.7±0.09	4.7±0.03	1.8±0.01	0.26±0.002
SS-EB	73±0.1	40.0±0.20	39.7±0.20	13.0±0.06	21.0±0.10	4.9±0.02	0.14±0.001
CS-EB	80±1.4	11.8±0.03	10.8±0.03	14.7±0.04	7.4±0.02	2.0±0.01	0.26±0.001
FS-EB	63±0.1	43.1±0.27	40.2±0.25	25.0±0.16	31.1±0.20	5.1±0.03	0.31±0.002
PS-AL	92.8±0.30	14.0±0.06	5.5±0.03	3.3±0.00	0.1±0.00	2.1±0.00	NA
AS-AL	75.9±0.24	37.4±0.03	48.7±0.03	25.3±0.03	0.7±0.00	3.9±0.01	NA
FS-AL	75.4±0.10	37.8±0.00	56.0±0.23	25.7±0.03	0.7±0.00	3.7±0.01	NA
PS-BF	81.7±0.52	18.2±0.07	23.1±0.11	24.3±0.09	2.1±0.02	2.6±0.01	0.1±0.00
SS-BF	72.2±0.0	42.3±0.12	41.4±0.02	24.0±0.17	1.4±0.01	6.8±0.00	0.1±0.00
DS-BF	65.0±0.0	24.7±0.03	30.8±0.09	44.5±0.03	3.5±0.03	3.7±0.02	0.2±0.00
FS-BF	61.3±0.1	25.3±0.03	32.8±0.34	44.7±0.00	3.5±0.01	3.6±0.00	0.2±0.00
SA-BF	0.7±0.0	75.0±0.12	34.0±0.06	99.1±0.18	11.4±0.03	14.8±0.09	0.5±0.00
PS-FR	78.6±0.3	30.5±0.14	33.4±0.22	27.9±0.03	3.6±0.03	3.6±0.02	0.3±0.00
AS-FR	76.7±0.1	39.3±0.13	25.6±0.17	15.6±0.19	6.8±0.04	6.8±0.00	0.2±0.00
SS-FR	75.8±0.2	39.4±0.17	26.1±0.08	15.5±0.06	6.9±0.03	6.9±0.00	0.2±0.00
TS-FR	69.6±0.4	45.1±0.11	36.5±0.09	20.7±0.11	8.4±0.03	8.4±0.00	0.2±0.00
BDS-FR	72.9±0.2	33.1±0.54	29.0±0.13	21.1±0.13	6.0±0.03	6.0±0.03	0.2±0.00
FS-FR	57.3±0.9	55.7±0.67	55.2±0.10	38.7±0.05	10.5±0.13	10.5±0.00	0.4±0.00

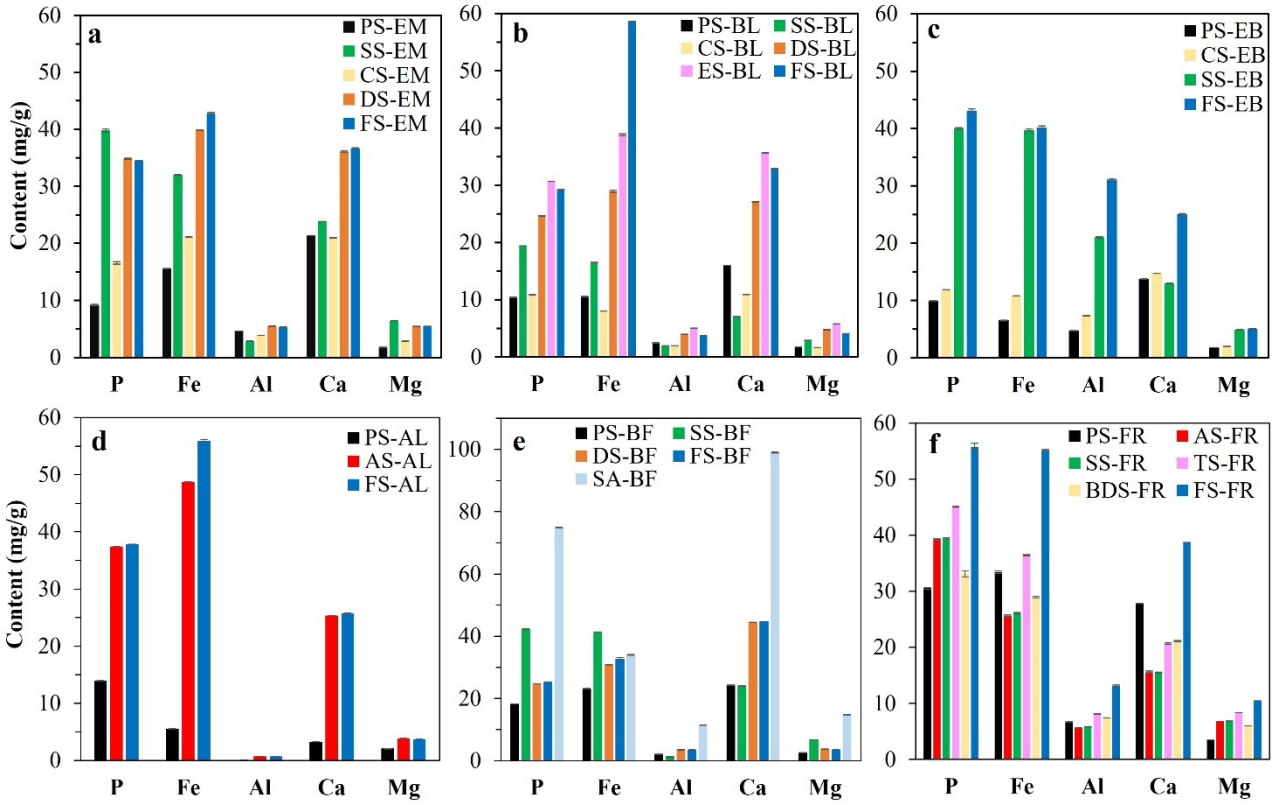

Fig. 2. Elemental analysis of the sludge samples from (a) Ejby Mølle, (b) Billund, (c) Esbjerg, (d) Arla, (e) Biofos, and (f) Fredericia WWTPs determined by ICP-OES based on dry weight.

2.2. Characterization of minerals in the sludge

Blue vivianite particles were observed visually for all sludge samples

Optical microscopy can visually examine the existence of vivianite in the target sample by the characteristic blue particles of vivianite (Prot et al., 2020; Rothe et al., 2016). As Fig. 3 shows, blue vivianite particles were observed in all the sludge samples in this study.

Vivianite is the only crystalline phosphate mineral observed, but only in some samples

PXRD probes the crystalline phases in the sludge samples. The PXRD diffractograms of the Ejby Mølle sludge reveal the presence of vivianite, calcite, and quartz (sand) in DS-EM and FS-EM,

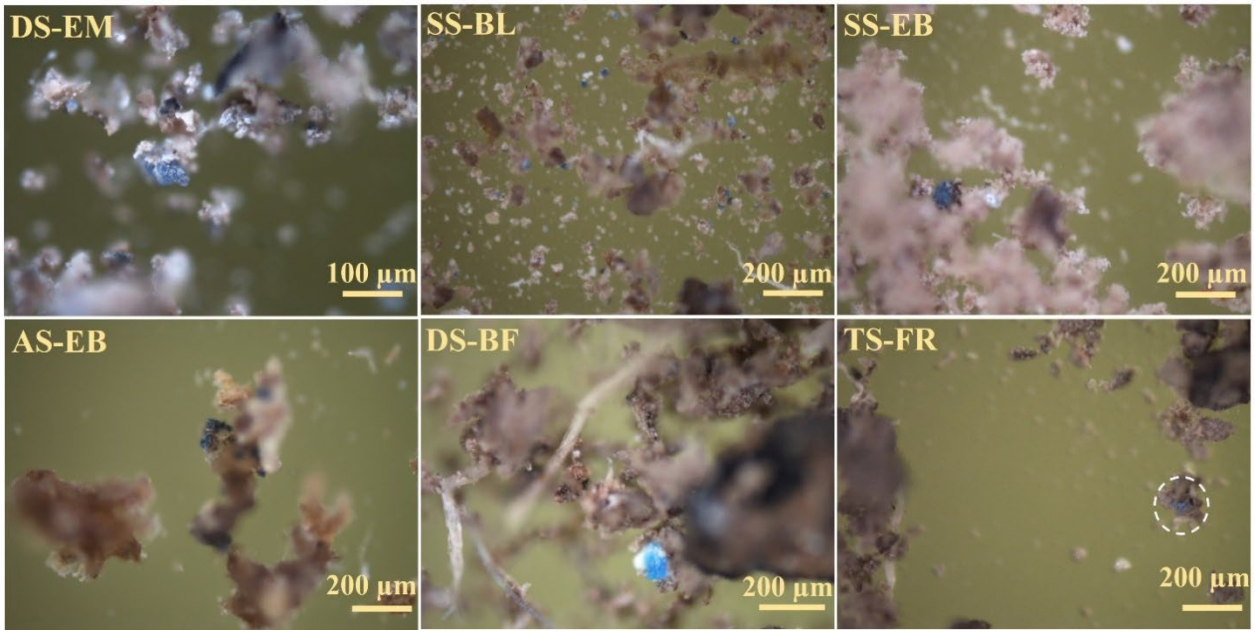

Fig. 3. Observation of blue vivianite particles in the sludge samples. One sludge sample from each WWTP has been selected.

whereas only calcite and quartz were the crystalline phases observed for other four EM sludge samples (Fig. 4a). For Billund sludge, reflections of vivianite and quartz were observed in SS-BL, DS-BL, and FS-BL, while quartz was present as the only crystalline phase in the other sludge samples (Fig. 4b). In Arla sludge, weak reflections of vivianite were observed in AS-AL and FS-AL, and no reflections of other crystalline phases were observed, so was for PS-AL (data not shown). Vivianite reflections as well as calcite and quartz were observedfor all the Biofos sludge samples except the sludge ash. PXRD diffractograms of sludge ash showed reflections from quartz, gypsum ($CaSO_4 \cdot 2H_2O$), whitlockite ($Ca_9(Mg)(PO_4)_6(PO_3OH)$), and hematite (Fe_2O_3). This suggests the conversion of Fe-P to Ca-P after the sludge incineration. For the Esbjerg and Fredericia sludge samples quartz were the main crystalline phase(data not shown), i.e., no crystalline vivianite.

Given the observation of blue vivianite particles in all the sludge samples by optical microscopy, the absence of vivianite reflections in the PXRD diffractograms should be attributed to

a low vivianite content and/or PXRD-amorphous ("X-ray invisible") vivianite(Wang et al., 2022). For example, the absence of crystalline vivianite in ES-BL was probably due to the structural degradation of vivianite during the Exelys^{TM} thermal treatment (160 ˚C, 30 min). It was reported that vivianite degradation was favored at high temperature, resulting in the formation of poorly crystalline mixed-valence Fe phosphate phases, e.g., lipscombite $(Fe(II)Fe(III)_2\ (PO_4)_2(OH)_2)$ (Rothe et al., 2016). The broad bumps at 2θ of 15-25˚ originate from biomass, which is commonly observed in PXRD diffractograms of sludge (Prot et al., 2020; Wilfert et al., 2018). Thus, PXRD, which is a fast analyses method, but it may provide a "false negative" about vivianite.

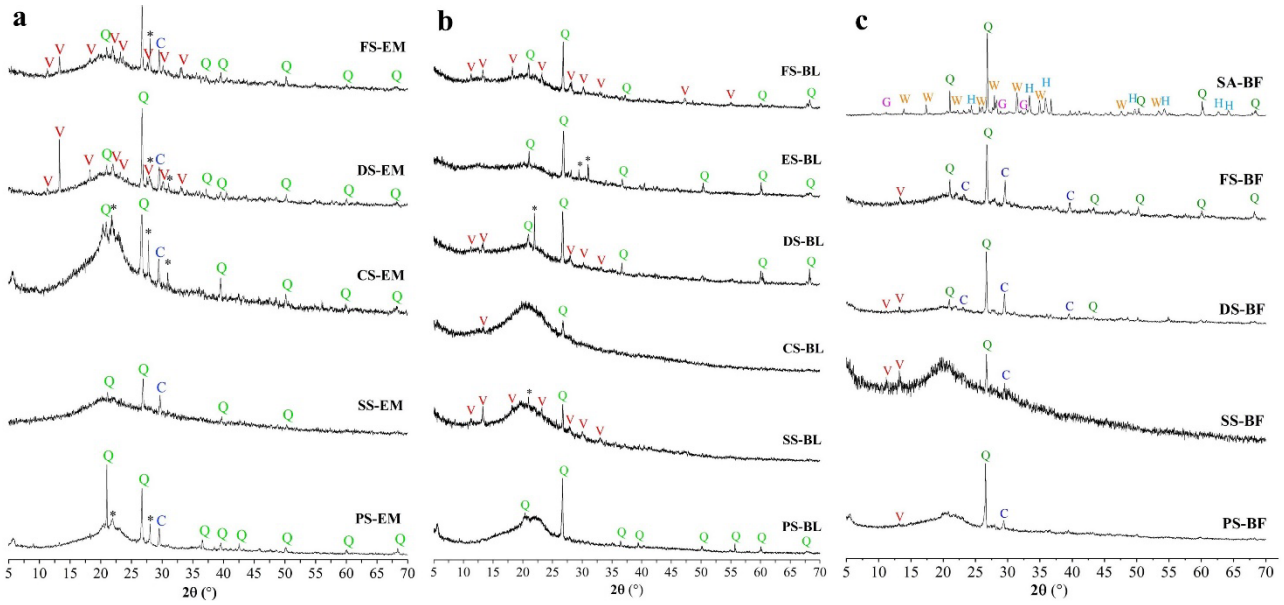

Fig. 4. PXRD diffractograms of the sludge samples from (a) Ejby Mølle, (b) Billund, and (c) Biofos. Q: quartz SiO_2, V: vivianite $Fe_3(PO_4)_2{\cdot}8H_2O$, C: calcite $CaCO_3$, G: gypsum $CaSO_4{\cdot}2H_2O$, W: whitlockite $Ca_9(Mg)(PO_4)_6(PO_3OH)$, H: hematite Fe_2O_3, *: unassigned.

Observation of vivianite by SEM-EDS in all sludge samples and amorphous Al-P in Al-dosed sludge

SEM-EDS examines morphological and elemental properties of the sludge samples. In all sludge samples, vivianite particles which are in an aggregate shape with overlapping P & Fe signals (Prot et al., 2019; Prot et al., 2020; Wilfert et al., 2016) were observed (Fig. 5), in agreement with the

findings by optical microscopy (see Fig. 3). EDS revealed molar Fe:P ratios of 1.1-1.6 in regions with both Fe and P present, in agreement with earlier reported EDS values of 1.0-1.6 (Wang et al., 2021) and 1.1-1.7 (Wilfert et al., 2016) for vivianite particles in sludge. Moreover, overlap of P & Fe & Mg was also observed for some vivianite particles reflecting substitution of Mg to a part of Fe in vivianite in the sludge samples (Wang et al., 2021; Wilfert et al., 2018). Esbjerg sludge after Al dosing (SS-EB and FS-EB) showed a homogenous distribution of Al and P almost across the entire sample surface (Fig. 5d as an example). This suggests the existence of amorphous Al-P, as no crystalline aluminum phosphates were identified by PXRD. Solid-state ^{27}Al MAS NMR revealed the existence of Al (hydr)oxides adsorbed with phosphate in Al-dosed Esbjerg sludge samples, i.e., SS-EB and FS-EB. Hence, phosphate adsorbed on amorphous Al (hydr)oxides (no reflection in PXRD) could be the main Al-P phase in the Esbjerg sludge after Al dosing.

Fig. 5 (following page). SEM images of (a) FS-EM, (b) SS-BL, (c) FS-EB, (e) FS-AL, and (f) FS-BL and the vivianite particles observed in them with overlapping P (in green) and Fe (in orange) signals by elemental mapping. (d) SEM of FS-EB with elemental mapping of P (in green) and Al (in blue). Vivianite particles were also identified in other sludge samples (data not shown).

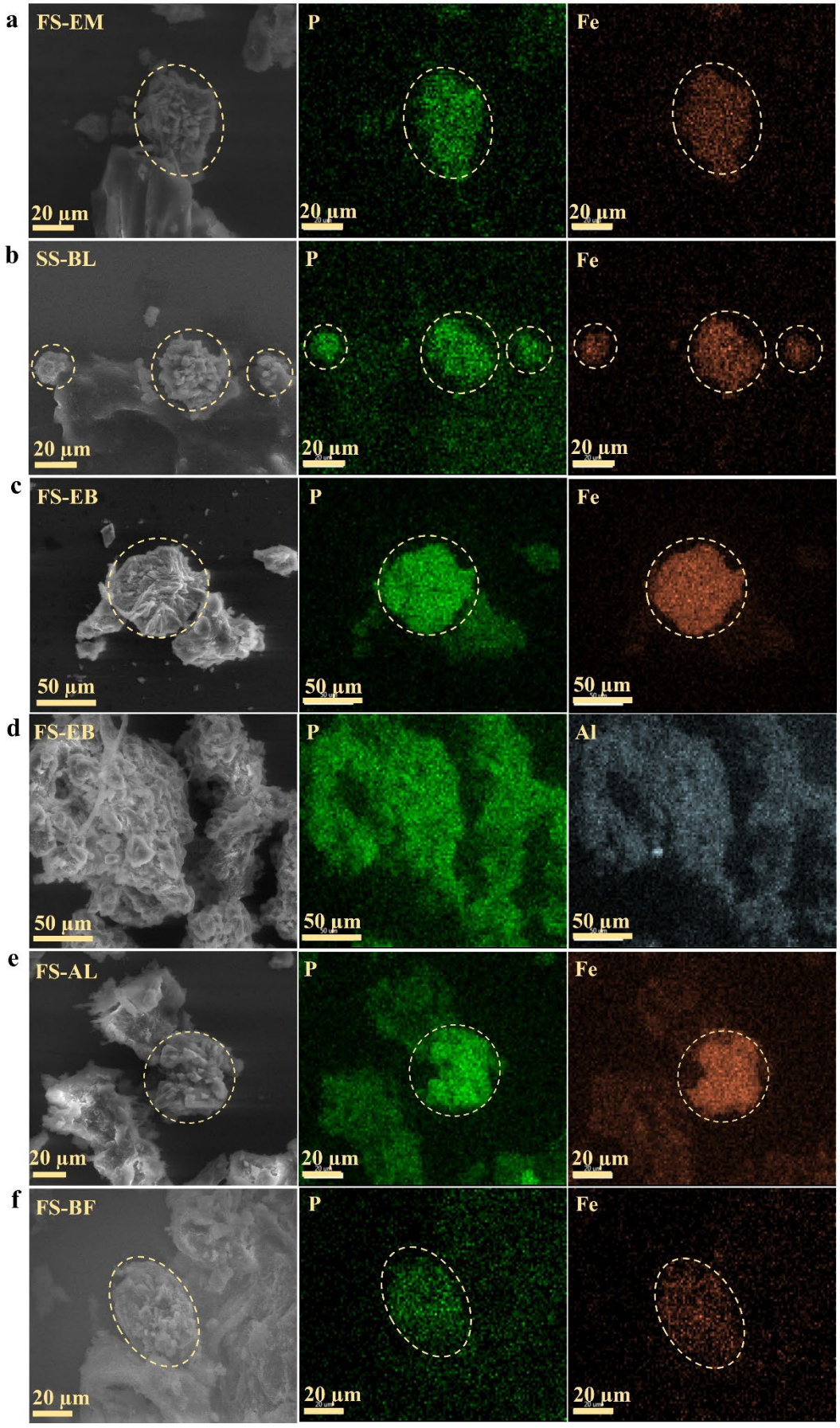
a
FS-EM
P
Fe
20 µm
20 µm
20 µm
b
SS-BL
P
Fe
20 µm
20 µm
20 µm
c
FS-EB
P
Fe
50 µm
50 µm
50 µm
d
FS-EB
P
Al
50 µm
50 µm
50 µm
e
FS-AL
P
Fe
20 µm
20 µm
20 µm
f
FS-BF
P
Fe
20 µm
20 µm
20 µm

3. Changes of the P species in the sludge throughout the WWTPs

Liquid-state ^{31}P NMR quantified the different P species in the sample including inorganic ortho-P, organic-P (e.g., phosphate monoester, phosphate diester, and phospholipids), poly-P, and pyro-P. The relative abundances of these fractions were estimated by spectral integration (Table 2 and Fig. 6).

As shown in Fig. 6a, inorganic ortho-P (53%) and organic-P (45%) were dominant with small quantities of pyro-P and poly-P (2% in total) in PS-EM. SS-EM contained the highest amount of poly-P (44%) as it is accumulated by PAOs in the enhanced biological P removal (EBPR) process, followed by inorganic ortho-P (41%) and organic-P (15%). CS-EM mainly contained inorganic ortho-P (62%), organic-P (26%), and poly-P (12%), as it is a mixture of external industrial waste and sludge from the primary and secondary tanks. Following anaerobic digestion, nearly all poly-P and most organic-P were degraded reflecting the conversion of biogenic P (bio-P) to inorganic ortho-P (> 90 % ortho-P) for DS-EM and FS-EM.

The same trend for the P species was observed at other WWTPs. Namely, primary sludge was dominated by inorganic ortho-P and organic-P in comparable amounts, whereas poly-P was formed after aerated biological treatment (i.e., in activated sludge and secondary sludge). Subsequently, poly-P and organic-P were degraded by anaerobic digestion, making inorganic ortho-P as the dominant P species in the downstream sludge.

Notably, Exelys^{M} thermal hydrolysis had an insignificant effect on the P species in the Billund sludge as DS-BL (before Exelys^{TM}) and ES-BL (Exelys^{TM}) had similar distribution of P species (Fig. 6b and Table 2). However, the thermal hydrolysis at Fredericia degraded most poly-P and organic-P, increasing the content of inorganic ortho-P from 38% to 92%. This reflects that the effect of thermal hydrolysis on P species in sludge is closely correlated with its location in the WWTP considering the composition of the incoming sludge. The higher abundance of poly-P in SS-EM and SS-FR than in

the secondary sludge of the four other WWTPs (44-45% vs 22-27%) suggests a better performance of the EBPR at Ejby Mølle and Fredericia WWTPs.

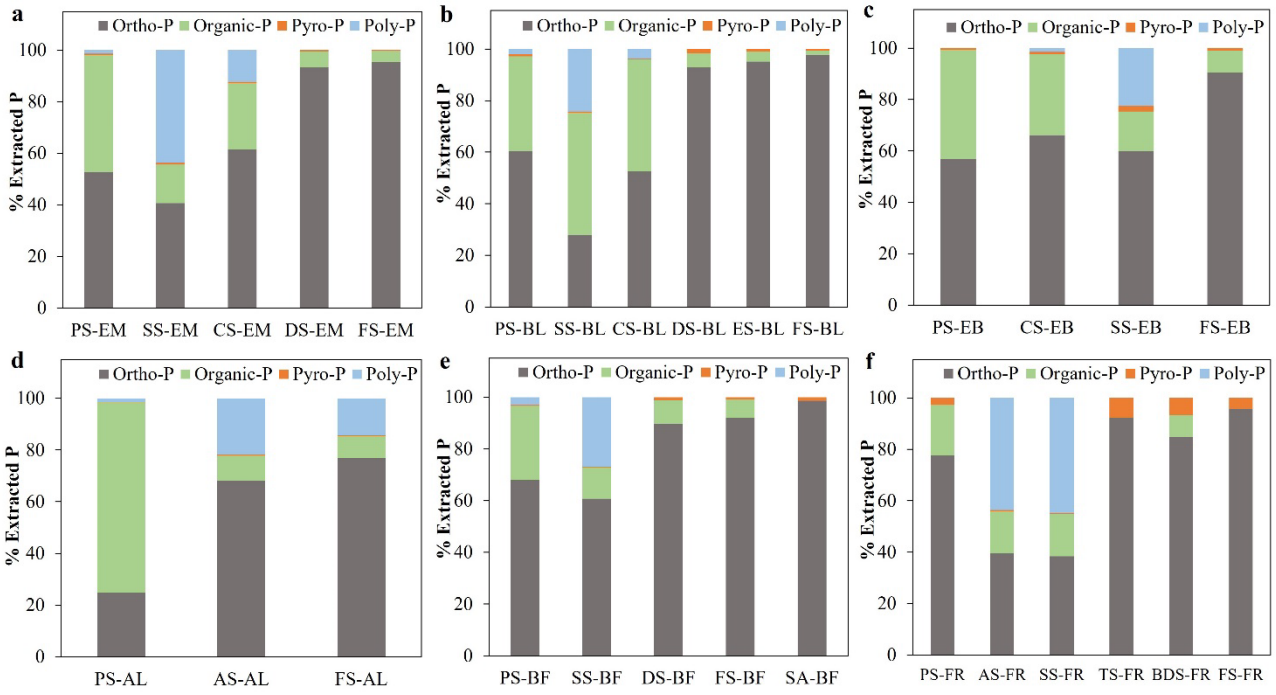

Fig. 6. Concentration of the different P species in the sludge samples from (a) Ejby Mølle, (b) Billund, (c) Esbjerg, (d) Arla, (e) Biofos, and (f) Fredericia WWTPs using liquid-state ^{31}P NMR spectroscopy.

Table 2 Concentrations of different P species in the sludge samples (% Extracted P) based on liquid-state ^{31}P NMR analysis.

	Inorganic ortho-P	Organic-P	Pyro-P	Poly-P
Ejby Mølle				
PS-EM	52.8	45.4	0.6	1.3
SS-EM	40.6	15.0	0.7	43.7
CS-EM	61.5	25.7	0.6	12.3
DS-EM	93.3	6.2	0.4	0.0
FS-EM	95.5	4.3	0.3	0.0
Billund				
PS-BL	60.5	36.6	0.9	2.0
SS-BL	27.9	47.3	0.5	24.3
CS-BL	52.5	43.5	0.3	3.7
DS-BL	92.9	5.4	1.7	0.0
ES-BL	95.1	3.9	1.0	0.0
FS-BL	97.8	1.6	0.6	0.0
Esbjerg				
PS-EB	56.9	42.3	0.8	0.0
CS-EB	66.1	31.6	0.9	1.5
SS-EB	59.9	15.4	2.2	22.5
FS-EB	90.5	8.5	1.0	0.0
Arla				
PS-AL	24.7	73.7	0.1	1.4
AS-AL	68.2	9.6	0.4	21.8
FS-AL	76.9	8.5	0.4	14.3
Biofos				
PS-BF	67.9	28.7	0.4	3.0
SS-BF	60.7	12.2	0.3	26.9
DS-BF	89.7	9.1	1.2	0.0
FS-BF	91.9	7.2	0.9	0.0
SA-BF	98.6	0	1.4	0
Fredericia				
PS-FR	77.6	19.6	2.8	0
AS-FR	39.5	16.4	0.5	43.6
SS-FR	38.3	16.6	0.4	44.8
TS-FR	92.2	0.2	7.7	0
BDS-FR	84.9	8.5	6.6	0
FS-FR	95.7	0	4.3	0

4. Quantification of the different P fractions in the inorganic ortho-P

The liquid-state ^{13}P NMR analysis shows that inorganic ortho-P is an important P species in the sludge, especially in sludge after anaerobic digestion. To quantify the different P fractions of the inorganic ortho-P, our sequential P extraction protocol (Wang et al., 2021) was employed for quantification of different P fractions in sludge. The fractions include loosely bound and porewater P (quantified as H_2O-P), vivianite-P (Bipy-P), Fe(III)-P (BD-P, i.e., ferric phosphate and P sorbed on Fe (oxyhydr)oxides), Al-P (NaOH-P), Ca- and Mg-bound P (HCl-P), residue-P, P bound to humic substances (humic-P), and non-reactive P (nrP, i.e., bio-P such as organic-P and poly-P) (Wang et al., 2021). As shown in Fig. 7 (details in Table 3), bio-P (nrP) had a higher portion in the sludge samples before anaerobic digestion especially in secondary sludge than in samples after anaerobic digestion, in agreement with the liquid-state ^{31}P NMR (Fig. 6). The following discussion focuses on inorganic ortho-P, e.g., Bipy-P, BD-P, NaOH-P, and HCl-P.

Ejby Mølle WWTP

Vivianite-P (Bipy-P) was the dominant inorganic ortho-P in the primary sludge from Ejby Mølle (31% TP; Fig. 7a). This implies the prevalent occurrence of vivianite formation at WWTPs via reaction of phosphate and Fe, which is dosed or present in the recirculated wastewater. A high vivianite-P content was also found in the secondary sludge (23% TP). This may reflect the rapid reduction of Fe(III) to Fe(II) in the micro anaerobic space formed in the secondary tank (Salehin et al., 2019). The existence of vivianite in secondary sludge has been reported earlier in other WWTPs. For example, vivianite-P accounted for 9-13% of TP at a WWTP applying Fe dosing and EBPR according to Mössbauer spectroscopy and PXRD (Wilfert et al., 2016). The sludge from the concentration tank was a mixture of primary sludge, secondary sludge, and external industrial sludge. Comparing it and the digested sludge, which was sludge before and after anaerobic digestion, respectively, the vivianite-P content was increased by 160% and the Fe(III)-P content increased by a factor of 4. This implies that more

Fe(II) was formed from Fe(III) reduction and favored vivianite formation under the anaerobic condition. The inorganic ortho-P from bio-P degradation was also bound to Fe(III), thereby generating Fe(III) phosphate and/or P sorbed on Fe(III) minerals. Overall, the content of Fe-P (i.e., vivianite-P + Fe(III)-P) in the sludge was increased from 46% to 71% of TP via anaerobic digestion.

Billund WWTP

The P fractions for the different Billund sludge samples were similar to the corresponding at Ejby Mølle sludge (Fig. 7 b and Table 3). The vivianite-P content increased by more than 200 % and the Fe(III)-P content by about 40 times after anaerobic digestion. Overall, Fe-P (i.e., vivianite-P + Fe(III)-P) in the sludge increased from 29% to 71% of TP via anaerobic digestion in Billund. Notably, the vivianite-P portion in the sludge decreased after Exelys^{TM}, i.e., from 32% in DS-BL to 22% in ES-BL (Fig. 7b). This should be ascribed to the degradation of vivianite (e.g., oxidation to Fe(III) phosphate) during the thermal treatment in Exelys^{TM}, which was supported by PXRD, optical microscopy, and SEM-EDS. This is also consistent with the higher portion of Fe(III)-P (BD-P) in ES-BL than in DS-BL (55% vs 38%, Fig. 7b).

Esbjerg WWTP

At Esbjerg WWTP, the concentration tank only collected the primary sludge, which was mixed with the secondary sludge in the anaerobic digester. This explains the similar P fractions in CS-EB and PS-EB (Fig. 7c). In SS-EB and FS-EB, which are located after Fe & Al dosing, the inorganic ortho-P was mainly consisted of vivianite-P (Bipy-P), Fe(III)-P (BD-P), and Al-P (NaOH-P). Notably, SS-EB showed a significant proportion of vivianite-P (30%), even higher than that of FS-EB (15%). Taking Fe(III)-P into account, Fe-P comprised 47% of TP in SS-EB and 38% of TP in FS-EB. In addition, SS-EB and FS-EB contained significant portions of Al-P due to Al dosing (17-38% TP) as compared with Billund and Ejby Mølle sludge (0.3-10% TP). This reflects the competition between Fe and Al for phosphate sequestration.

Arla WWTP

As Fig. 7d shows, the primary sludge (PS-AL, the solid part of the dairy-processing wastewater) was dominated by bio-P (78%), the rest is loosely bound and porewater P. The activated sludge (AS) and final sludge (FS) contained comparable amounts of vivianite-P (24%), Fe(III)-P (35-43%), and bio-P (25-35%). Thus, Fe-P, which includes vivianite-P and Fe(III)-P, was the dominant inorganic P species in the Arla sludge.

Biofos WWTP

A similar trend in the P fractions was observed throughout the Biofos WWTP as for Ejby Mølle and Billund WWTPs (Fig. 7e). Again, Fe-P (vivianite-P + Fe(III)-P) was the dominant inorganic P phase in the sludge, accounting for 63%, 45%, 62%, and 73% of TP in PS, SS, DS, and FS, respectively. After incineration, the HCl-P pool became the dominant (83%, which mainly reflects Ca-P given the much higher content of Ca than Mg, see Table 1 and Fig.2). This suggests the conversion of Fe-P to Ca-P during sludge incineration accompanied by the formation of hematite. This is supported by the PXRD diffractograms, where quartz, vivianite ($Fe_3(PO_4)_2{\cdot}8H_2O$), and calcite ($CaCO_3$) are the main crystalline phases in FS-BF (before incineration), whereas quartz, whitlockite ($Ca_9(Mg)(PO_4)_6(PO_3OH)$), hematite (Fe_2O_3), and gypsum ($CaSO_4{\cdot}2H_2O$) are observed after incineration (SA-BF).

Fredericia WWTP

The AS-FR and SS-FR had high contents of bio-P (nrP, 59-66% of TP), which should be attributed to poly-P (Fig 7f). Vivianite-P (Bipy-P) was the dominant inorganic ortho-P in the sludge samples and accounted for 30-57% of TP (Table 3). The presence of vivianite in the sludge was verified by the characteristic blue vivianite particles observed by optical microscopy (Fig. 3). However, no significant reflections of vivianite were observed by PXRD (data not shown), suggesting that the vivianite in the sludge samples were X-ray amorphous. The high content of loosely bound and porewater P (H_2O-P, 34%) in TS-FR indicates the release of phosphate from bio-P after thermal

hydrolysis. After anaerobic digestion, the Fe(III)-P content was increased from 11% (BDS-FR) to 23% (FS-FR), indicating that the P released from bio-P degradation during anaerobic digestion was sequestered by Fe(III).

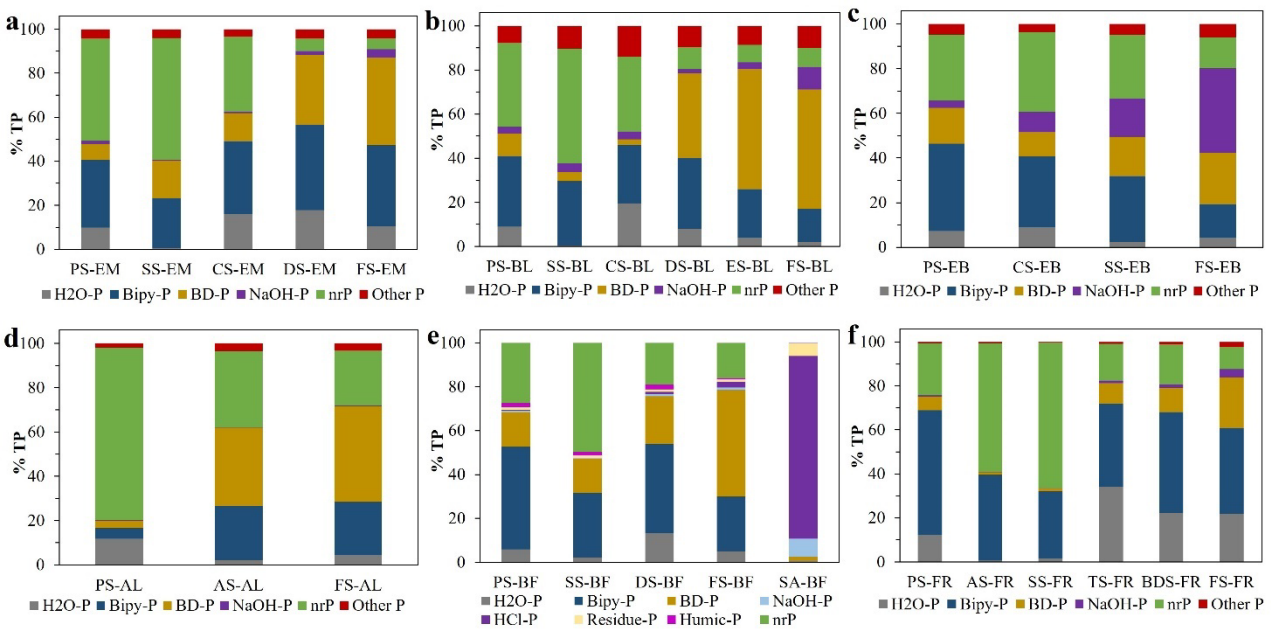

Fig. 7. Relative concentration of the different P fractions in the sludge samples from (a) Ejby Mølle, (b) Billund, (c) Esbjerg, (d) Arla, (e) Biofos, and (f) Fredericia WWTPs determine by sequential P extraction. HCl-P, Residue-P, and Humic-P are combind as "Other-P" for WWTPs except Biofos due to their small proportions. The individual concentrations are given in Table 3.

Table 3 Proportions of different P fractions in the sludge using sequential P extraction (% of TP).

	H_2O-P	Bipy-P	BD-P	NaOH-P	HCl-P	Residue-P	Humic-P	nrP
Ejby Mølle WWTP								
PS-EM	9.9	30.7	7.3	1.5	1.4	1.2	1.8	46.4
SS-EM	0.5	22.7	17.2	0.3	0.1	1.8	2.1	55.3
CS-EM	15.9	33.2	12.8	0.6	0.3	1.2	2.0	34.0
DS-EM	17.8	38.9	31.7	1.7	0.8	1.5	2.0	5.7
FS-EM	10.4	36.8	39.7	3.9	0.9	1.0	2.2	5.0
Billund WWTP								
PS-BL	9.0	31.9	10.4	2.9	2.7	2.0	3.1	38.1
SS-BL	0.3	29.3	4.1	4.0	0.2	3.8	6.3	52.0
CS-BL	19.5	26.5	2.5	3.5	0.2	7.3	6.5	34.0
DS-BL	8.0	32.1	38.4	2.0	3.5	4.3	1.9	9.8
ES-BL	3.9	21.9	54.5	3.1	6.2	2.0	0.4	7.9
FS-BL	2.0	15.0	54.2	10.1	6.9	1.6	1.5	8.7
Esbjerg WWTP								
PS-EB	7.3	39.2	16.0	3.1	1.4	1.0	2.3	29.7
CS-EB	8.9	31.7	10.9	9.1	0.6	0.9	2.1	35.7
SS-EB	2.4	29.5	17.7	17.2	0.2	1.1	3.5	28.5
FS-EB	4.2	15.1	23.2	37.8	1.0	0.8	4.1	13.9
Arla WWTP								
PS-AL	11.9	4.7	3.4	0.3	0.2	0.6	1.1	77.9
AS-AL	2.3	24.3	35.3	0.2	0.1	1.4	1.9	34.5
FS-AL	4.4	24.1	43.2	0.3	0.1	1.3	1.9	24.8
Biofos WWTP								
PS-BF	5.9	46.8	15.7	0.7	0.4	1.2	1.8	27.5
SS-BF	2.2	29.5	15.6	0.3	0.2	0.9	1.6	49.8
DS-BF	13.3	40.6	21.8	1.0	1.0	1.1	2.1	19.1
FS-BF	5.1	24.9	48.5	1.2	2.6	1.0	0.5	16.1
SA-BF	0.7	NA	1.8	8.2	83.3	5.7	0.1	0.2
Fredericia WWTP								
PS-FR	12.2	56.7	6.2	0.7	0.3	0.1	0.2	23.6
AS-FR	0.6	39.0	1.2	0.2	0.1	0.3	0.2	58.5
SS-FR	1.5	30.5	1.3	0.1	0.1	0.2	0.1	66.2
TS-FR	34.2	37.7	9.3	1.1	0.7	0.2	0.1	16.8
BDS-FR	22.4	45.7	11.0	1.6	0.8	0.2	0.3	18.0
FS-FR	21.8	39.0	23.0	3.7	1.5	0.3	0.5	10.1

5. Summary

(1) Vivianite was present in all the sludge samples, but crystalline vivianite (PXRD visible) was usually observed in the sludge after anaerobic digestion, and sometimes in secondary sludge.

(2) Inorganic ortho-P and organic-P were the main P species in primary sludge and of comparable size. Significant poly-P was present only in the secondary sludge (up to 45%) due to the EBPR process, where poly-P is accumulated by PAOs. After anaerobic digestion, poly-P and organic-P were degraded, making inorganic ortho-P as the dominant P in the downstream sludge (> 90%).

(3) For all Fe-dosing WWTPs, Fe-P (i.e., vivianite-P + Fe(III)-P) was the dominant inorganic ortho-P, and the concentration increased following anaerobic digestion. For Esbjerg sludge, Fe-P was also the dominant inorganic ortho-P in the primary sludge (55% of TP), but Al dosing rendered Al-P (i.e., P sorbed on amorphous Al (hydr)oxides) a significant fraction of inorganic ortho-P in secondary (17% of TP as Al-P, 47% of TP as Fe-P) and final sludge (38% of TP as Al-P, 38% of TP as Fe-P). The co-dosing of Al and Fe at Esbjerg WWTP led to competition between Al and Fe for phosphate.

(4) The Exelys^{TM} thermal hydrolysis process showed insignificant effect on the P speciation in Billund sludge, but it could degrade vivianite and result in a poorly crystalline structure. At Fredericia where the thermal hydrolysis treatment is after the secondary tank, the organic-P and poly-P in the secondary sludge were degraded into inorganic ortho-P after thermal hydrolysis.

(5) Sludge incineration could make the phosphate bound to Fe transfer to Ca, resulting in Ca-P (83% TP) as the dominant P in the sludge ash of Biofos.

Nomenclature

AL	Arla
AS	Activated sludge
BD	Bicarbonate dithionite solution used for Fe(III)-P extraction
BDS	Sludge before digestion
Bipy	Bipyridine solution used for vivianite extraction
BL	Billund
BF	Biofos
Bio-P	Biogenic P
CPR	Chemical P removal
CS	Sludge from concentration tank
DS	Digested sludge from anaerobic digester
EB	Esbjerg
EBPR	Enhanced biological P removal
EDS	Energy dispersive X-ray spectroscopy
EM	Ejby Mølle
ES	Exelys^{TM} sludge
FR	Fredericia
FS	Final sludge
ICP-OES	Inductively coupled plasma-optical emission spectroscopy
LOI	Loss on ignition
MAS	Magic-angle spinning
NMR	Nuclear magnetic resonance
nrP	non-reactive P, i.e., bio-P
Organic-P	Organophosphate
Ortho-P	Orthophosphate
Poly-P	Polyphosphate
Pyro-P	Pyrophosphate
PS	Primary sludge
PXRD	Powder X-ray diffraction
SA	Sludge ash
SEM	Scanning electron microscopy
SS	Secondary sludge
TP	Total P
TS	Thermal hydrolysis sludge
WWTP	wastewater treatment plant

References

Prot, T., Nguyen, V.H., Wilfert, P., Dugulan, A.I., Goubitz, K., De Ridder, D.J., Korving, L., Rem, P., Bouderbala, A., Witkamp, G.J. and van Loosdrecht, M.C.M. 2019. Magnetic separation and characterization of vivianite from digested sewage sludge. Separation and Purification Technology 224, 564-579.

Prot, T., Wijdeveld, W., Eshun, L.E., Dugulan, A., Goubitz, K., Korving, L. and Van Loosdrecht, M. 2020. Full-scale increased iron dosage to stimulate the formation of vivianite and its recovery from digested sewage sludge. Water Research, 115911.

Rothe, M., Kleeberg, A. and Hupfer, M. 2016. The occurrence, identification and environmental relevance of vivianite in waterlogged soils and aquatic sediments. Earth-Science Reviews 158, 51-64.

Salehin, S., Kulandaivelu, J., Rebosura, M., Khan, W., Wong, R., Jiang, G.M., Smith, P., McPhee, P., Howard, C., Sharma, K., Keller, J., Donose, B.C., Yuan, Z.G. and Pikaar, I. 2019. Opportunities for reducing coagulants usage in urban water management: The Oxley Creek Sewage Collection and Treatment System as an example. Water Research 165.

Wang, Q., Kim, T.-H., Reitzel, K., Almind-Jørgensen, N. and Nielsen, U.G. 2021. Quantitative determination of vivianite in sewage sludge by a phosphate extraction protocol validated by PXRD, SEM-EDS and 31P NMR spectroscopy towards efficient vivianite recovery. Water Research, 117411.

Wang, Q., Raju, C.S., Almind-Jørgensen, N., Laustrup, M., Reitzel, K. and Nielsen, U.G. 2022. Variation in Phosphorus Speciation of Sewage Sludge throughout Three Wastewater Treatment Plants: Determined by Sequential Extraction Combined with Microscopy, NMR Spectroscopy, and Powder X-ray Diffraction. Environmental Science & Technology.

Wilfert, P., Dugulan, A.I., Goubitz, K., Korving, L., Witkamp, G.J. and Van Loosdrecht, M.C.M. 2018. Vivianite as the main phosphate mineral in digested sewage sludge and its role for phosphate recovery. Water Research 144, 312-321.

Wilfert, P., Mandalidis, A., Dugulan, A.I., Goubitz, K., Korving, L., Temmink, H., Witkamp, G.J. and Van Loosdrecht, M.C.M. 2016. Vivianite as an important iron phosphate precipitate in sewage treatment plants. Water Research 104, 449-460.